30/129189 9-5 (3)

CONF-890335--202

SLAC-PUB-4907
March 1989
(A)

ONLINE MONITORING OF DISPERSION FUNCTIONS AND TRANSFER MATRICES AT THE SLC+

P. EMMA, T. H. FIEGUTH, T. LOHSE
Stanford Linear Accelerator Center, Stanford University, Stanford, California 94309
P. R. BURCHAT*
University of California, Santa Cruz, California 95064
R. S. PANVINI**
Vanderbuilt University, Nashville, Tennessee 37235

SLAC-PUB--4907
DE89 013745

ABSTRACT

The symmetries of the chromatic correction sections in the SLC Final Focus System allow a high-resolution determination of the pulse-to-pulse energy fluctuations by exploiting the information from beam position monitors (BPMs) in regions of large dispersion. By correlating this signal with other BPMs, one can infer the dispersion function as well as spatial components of transfer matrices anywhere in the arcs and the Final Focus System without interrupting normal machine operation. We present results from data recorded during either periods of stable operation or periods when the linac energy was intentionally varied.

1. INTRODUCTION

The Final Focus System (FFS)[1,2] in the Stanford Linear Collider (SLC) is a complex optical system for strong demagnification of beams at the interaction point. This requires not only a careful minimization of higher-order aberrations using a dedicated chromatic correction section (CCS),[3] sketched in Fig. 1, but also a precise matching of the dispersion function at the entrance of the FFS. The input dispersion is measured by varying the energy in the linac and recording the correlated beam motion at strip-line beam position monitors (BPMs) in the FFS. An online matching package[4] fits the results and predicts the strengths of four corrector quadrupoles in the FFS. This is an efficient tool for dispersion *correction* but is not suited for dispersion *monitoring* because it interrupts normal operation. In this paper we describe a complementary scheme which permits an online nondisruptive measurement of dispersion functions by exploiting natural fluctuations of the beam energy. This allows, for the first time, monitoring of the *stability* of the dispersion match. The scheme is based on the information of CCS BPMs at positions where both dispersion and β functions are large; i.e., BPMs with high sensitivity to energy and orbit fluctuations.

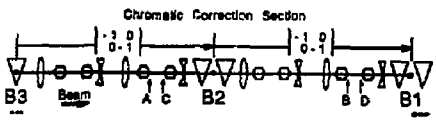

Fig. 1: Schematic of the CCS with positions of BPMs — (A), (B), (C) and (D) — indicated.

2. GEOMETRIC AND CHROMATIC COMPONENTS

We use TRANSPORT[5] notation to represent propagation of a beam from point (A) to point (B),

$$X^{(B)} = R_{11}X^{(A)} + R_{12}X'^{(A)} + R_{16}\delta \quad , \qquad (1)$$

where X is the transverse beam position, X' is the beam angle with respect to the design trajectory, and δ ($\equiv \Delta p/p$) is the fractional beam momentum deviation, which we identify with the fractional energy deviation since SLC beams are ultrarelativistic. $\mathbf{R}$ is the transfer matrix from point (A) to point (B), with X–Y coupling neglected.

The CCS is designed to correct lowest-order chromatic aberrations using 4-dipole, 8-quadrupole, and 8-sextupole magnets as shown in Fig. 1. These are arranged as two identical $-\mathbf{I}$ telescopes such that local geometric aberrations due to sextupoles are cancelled. Given this symmetry, the two-by-two beam transfer matrix from BPM (A) in the first telescope to BPM (B) in the second (see Fig. 1) is the negative identity matrix. This holds for both transverse planes. From (1) and $\mathbf{R}^{(A:B)} = -\mathbf{I}$, a simple relation for the beam energy deviation is found:

$$\delta = \frac{X^{(A)} + X^{(B)}}{R_{16}} \quad . \qquad (2)$$

The R_{16} element from BPM (A) to BPM (B) is large and well known (460 mm), since it is almost completely determined by the two CCS dipoles B2 in Fig. 1.

The position at BPM (A) or (B) can be decomposed into a pure betatron component (independent of δ), X_β, and a pure dispersive component,

$$X^{(A)} = X_\beta + \eta^{(A)}\delta \quad , \quad X^{(B)} = -X_\beta + \eta^{(B)}\delta \quad , \qquad (3)$$

where we again use $\mathbf{R}^{(A:B)} = -\mathbf{I}$. Now we define ΔX as the difference between the BPM readings:

$$\Delta X \equiv \frac{1}{2}\left(X^{(A)} - X^{(B)}\right) = X_\beta + \Delta\eta\,\delta \quad , \qquad (4)$$

where $\Delta\eta \equiv (1/2)(\eta^{(A)} - \eta^{(B)})$ represents the component of the dispersion at BPM (A) due to an upstream mismatch. In order to separate X_β from δ in Eq. (4), we assume $\Delta\eta$ is not time dependent over one set of measurements and calculate it from the correlation of δ with ΔX.

$$X_\beta = \Delta X - \frac{\langle \Delta X\,\delta\rangle}{\langle\delta^2\rangle}\delta \quad . \qquad (5)$$

The measurement of trajectory angles at BPMs (A) and (B) require the information of another pair of BPMs in the CCS, indicated by the labels (C) and (D) in Fig. 1. They are separated from BPMs (A) and (B) by simple drifts of known length $\Delta s \approx 2.4$ m.

$$X'^{(A)} = \frac{X^{(C)} - X^{(A)}}{\Delta s} \quad \text{and} \quad X'^{(B)} = \frac{X^{(D)} - X^{(B)}}{\Delta s} \qquad (6)$$

This allows a derivation of $\Delta X'$, X'_β and $\Delta\eta'$ in analogy to Eqs. (4) and (5).

A careful study of uncertainties in the CCS optics showed that systematic errors in these measurements are small and that the resolutions are sufficient for online monitoring.

3. BPM DATA ACQUISITION

An offline FORTRAN data acquisition program has been written to gather data from BPMs throughout the SLC and

† Work supported by the Department of Energy, contract DE-AC03-76SF00515.
* Work supported by the Department of Energy, contract DE-AM03-76SF00010.
** Work supported by the National Science Foundation.

Presented at the IEEE Particle Accelerator Conference, Chicago, Illinois, March 20–23, 1989.

MASTER DISTRIBUTION OF THIS DOCUMENT IS UNLIMITED

write it to disk. The X position, Y position, and beam intensity is sampled for 850 BPMs [including the CCS BPMs (A), (B), (C) and (D)] once every few seconds. The sample rate is one sample every ≈ 5 seconds. Presently, data is collected interactively over short periods, with 100 samples saved to disk for subsequent analysis. In the future, monitoring will run continuously, with data stored in a circular buffer. We will also store dynamically updating moments of BFM data for fast online fitting of lattice parameters, as described in the next chapter.

4. A MONITORING APPLICATION

The correlation of measured betatron fluctuations X_β and energy fluctuations δ with position measurements of BPMs in any region of interest can be exploited for a fast measurement of the dispersion function and elements of the transfer matrix. Let $X^{(i)}$ be the beam position measured at any BPM [labelled "(i)"]. Using Eq. (1) and the definition of X_β and X'_β, we can interpret this quantity in two ways:

$$X^{(i)} = R_{11}^{(A:i)} X^{(A)} + R_{12}^{(A:i)} X'^{(A)} + R_{16}^{(A:i)} \delta \quad (7a)$$

$$\text{or} \quad X^{(i)} = R_{11}^{(A:i)} X_\beta + R_{12}^{(A:i)} X'_\beta + \eta^{(i)} \delta \ . \quad (7b)$$

Both equations allow measurement of the transfer-matrix elements $R_{11}^{(A:i)}$ and $R_{12}^{(A:i)}$. The energy correlations, however, determine the *lattice* dispersion $R_{16}^{(A:i)}$ between BPMs (A) and (i) in (7a), but the dispersion *function* $\eta^{(i)}$ [*i.e.*, the total dispersion between the source of energy jitter and BPM (i)] in (7b). Therefore, (7b) is most useful for judgement of the total dispersion mismatch at the entrance of the FFS, while (7a) allows investigation of local lattice dispersion near the CCS and sources of mismatches within the FFS.

In Fig. 2, we present a simulation of this procedure. We generated 100 trajectories with energy fluctuations of 0.4% and relatively large betatron motions of four times the betatron size of the beam. All BPM readings were smeared according to a resolution of 20 μm. The results from properly error weighted fits[6] to (7a) and (7b) are in good agreement with the input lattice for all BPMs inside the FFS.

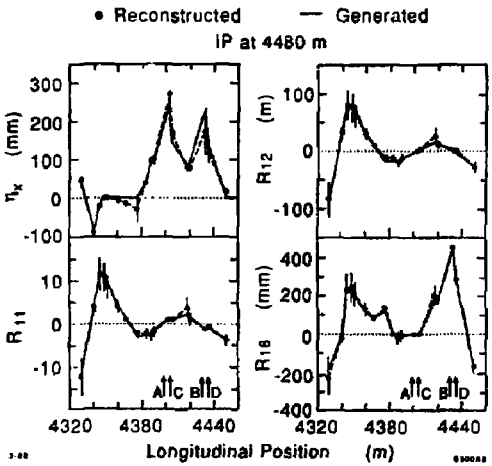

Fig. 2: Reconstructed FFS lattice parameters from simulated BPM data for 100 orbits with varying energies and trajectories.

Reducing the amplitude of the betatron fluctuation, however, quickly leads to resolution limitations for many of the FFS BPMs. It is therefore useful to reduce the number of fitted parameters in (7a) and (7b). One possibility is to average the measurements over the angular information at BPM (A):

$$\langle X^{(i)} \rangle|_{X^{(A)},\delta} = \left[R_{11}^{(A:i)} + \frac{\partial X'^{(A)}}{\partial X^{(A)}} R_{12}^{(A:i)} \right] X^{(A)} + \left[R_{16}^{(A:i)} + \frac{\partial X'^{(A)}}{\partial \delta} R_{12}^{(A:i)} \right] \delta \quad (8a)$$

$$\langle X^{(i)} \rangle|_{X_\beta,\delta} = \left[R_{11}^{(A:i)} + \frac{\partial X'_\beta}{\partial X_\beta} R_{12}^{(A:i)} \right] X_\beta + \eta^{(i)} \delta \quad (8b)$$

It is thus possible to measure $\eta^{(i)}$ and linear combinations of $R_{11}^{(A:i)}$ and $R_{12}^{(A:i)}$, or $R_{16}^{(A:i)}$ and $R_{12}^{(A:i)}$ with (8a) and (8b), respectively. The correlation parameters in these linear combinations can in principle be extracted from the data if they are stable during a single monitoring period.

Figure 3 shows the correlation terms in (8a) reconstructed from data taken during normal operation. The measurements are in good agreement with a linear combination of $R_{11}^{(A:i)}$ and $R_{12}^{(A:i)}$, or $R_{16}^{(A:i)}$ and $R_{12}^{(A:i)}$, which were obtained from fits of the nominal lattice parameters to the data and are superimposed in the figure.

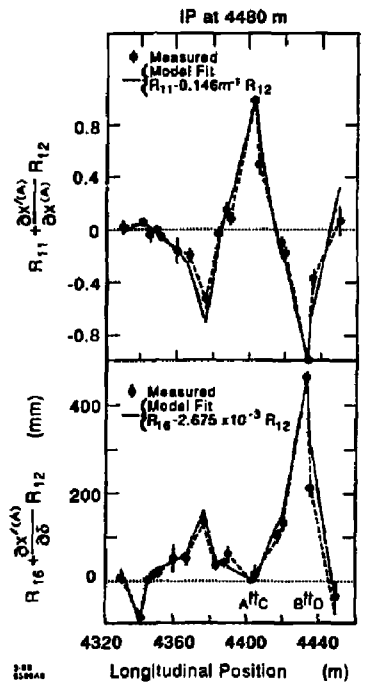

Fig. 3: Linear combinations of FFS lattice parameters from two-paramter fits to data taken during normal operation. Solid lines are best fits to data using design parameters.

Finally, averaging (8a) and (8b) over all betatron fluctuations yields a direct relation for the dispersion function:

$$\langle X^{(i)} \rangle|_\delta = \eta^{(i)} \delta \quad (9)$$

This simple one-parameter relation allows very stable fits. Fig. 4 shows the measurement of the dispersion function in the FFS

DISCLAIMER

This report was prepared as an account of work sponsored by an agency of the United States Government. Neither the United States Government nor any agency thereof, nor any of their employees, makes any warranty, express or implied, or assumes any legal liability or responsibility for the accuracy, completeness, or usefulness of any information, apparatus, product, or process disclosed, or represents that its use would not infringe privately owned rights. Reference herein to any specific commercial product, process, or service by trade name, trademark, manufacturer, or otherwise does not necessarily constitute or imply its endorsement, recommendation, or favoring by the United States Government or any agency thereof. The views and opinions of authors expressed herein do not necessarily state or reflect those of the United States Government or any agency thereof.

taken when the beam energy was intentionally varied by ±0.3%. This precision measurement reveals a dispersion mismatch at the entrance of the FFS. This is confirmed in Fig. 5, which shows the correlation of ΔX with δ, which according to Eq. (4)

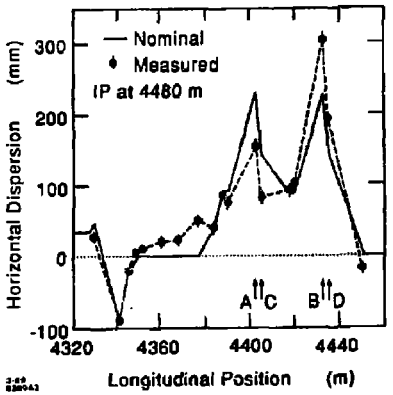

Fig. 4: Dispersion function in the FFS obtained from data with large energy fluctuations intentionally introduced.

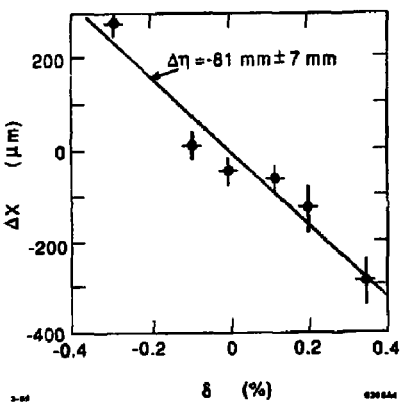

Fig. 5: Fit of the dispersion mismatch at BPM (A) for the data used in Fig. 4.

is the dispersion mismatch at BPM (A). The dispersion function in the arc was derived for the same data set and is displayed in Fig. 6. An example of a measurement of the FFS dispersion function taken during normal operation is presented in Fig. 7. The resolution of the measurement is satisfactory, although the dispersion function is derived solely from natural fluctuations in the beam energy.

5. PRESENT HARDWARE LIMITATIONS

At present, the range of applications for this scheme is limited, since most of the BPMs in the arcs and the FFS are read out in a multiplexed mode. Only a fraction of the available BPMs are read on the same beam pulses as BPMs (A) and (B), which define the energy fluctuation via (2). This influences the dispersion measurements in a systematic way if the natural energy fluctuations follow a fixed pattern in time. Similar limitations exist for the measurements of betatron orbit fluctuations.

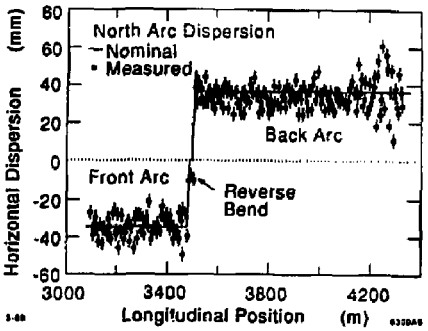

Fig. 6: As Fig. 4, for the north arc.

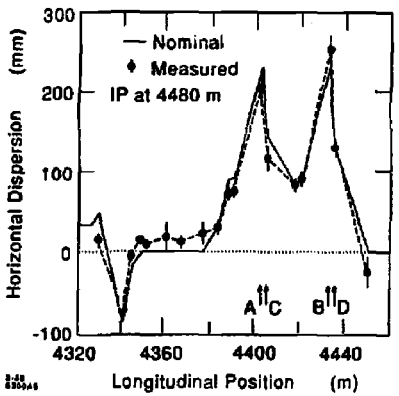

Fig. 7: As Fig. 4, for data taken during normal operation.

We plan to modify software and hardware such that information for BPMs (A), (B), (C) and (D) is available on all pulses of a multiplexer scan. This will further increase applicability of the new monitoring scheme.

ACKNOWLEDGMENTS

We would like to thank R. Grey, N. Phinney and B. Traller for their help in setting up hardware and software. We are indebted to A. Hutton and W. Kozanecki for their enthusiastic support and many helpful discussions. One of us (T. L.) was supported by a grant from the Max Kade Foundation.

REFERENCES

1. *SLC Design Handbook*, SLAC (December 1984).
2. J. J. Murray, K. L. Brown and T. Fieguth, "The Completed Design of the SLC Final Focus System," *Proc. Particle Accelerator Conference*, Washington D.C., Vol. 3, (1987) p. 1331; SLAC-PUB-4219 (February 1987).
3. K. L. Brown, *A Conceptual Design of Final Focus Systems for Linear Colliders*, SLAC-PUB-4159 (June 1987).
4. C. M. Hawkes and P. S. Bambade, "First Order Optical Matching in the Final Focus Section of the SLAC Linear Collider," *Nucl. Inst. and Meth.* **A274** (1989) 27.
5. K. L. Brown, F. Rothacker, D. C. Carey, and Ch. Iselin, *TRANSPORT, A Computer Program for Designing Charged Particle Beam Transport Systems*, SLAC-91, Rev. 2 (May 1977); Fermilab Report No. 91, CERN 80-04.
6. T. Lohse, P. Emma, *Linear Fitting of BPM Orbits and Lattice Parameters*, SLAC CN-371 (February 1989).